Electronic Supplementary Material (ESI) for Journal of Materials Chemistry C.

Supporting Information

High Linearity and Energy-Efficient Artificial Synaptic Device Based on Scalable Synthesized MoS_2

Yuxin Zhao[1,2], Yuanhao Jin[1,2], Xing Wang[1,2], Jie Zhao[1,2], Sanming Wu[1,2], Mengjuan Li[1,2], Jiaping Wang[1,2], Shoushan Fan[1,2], and Qunqing Li[1,2]**

[1]State Key Laboratory of Low-Dimensional Quantum Physics, Department of Physics & Tsinghua-Foxconn Nanotechnology Research Center, Tsinghua University, Beijing 100084, China

[2]Collaborative Innovation Center of Quantum Matter, Beijing, China

*Corresponding author. Tel.: +86 10 62796019; Fax: +86 10 62792457.

E-mail address: QunqLi@mail.tsinghua.edu.cn

S1. Characterization of MoS_2 film.

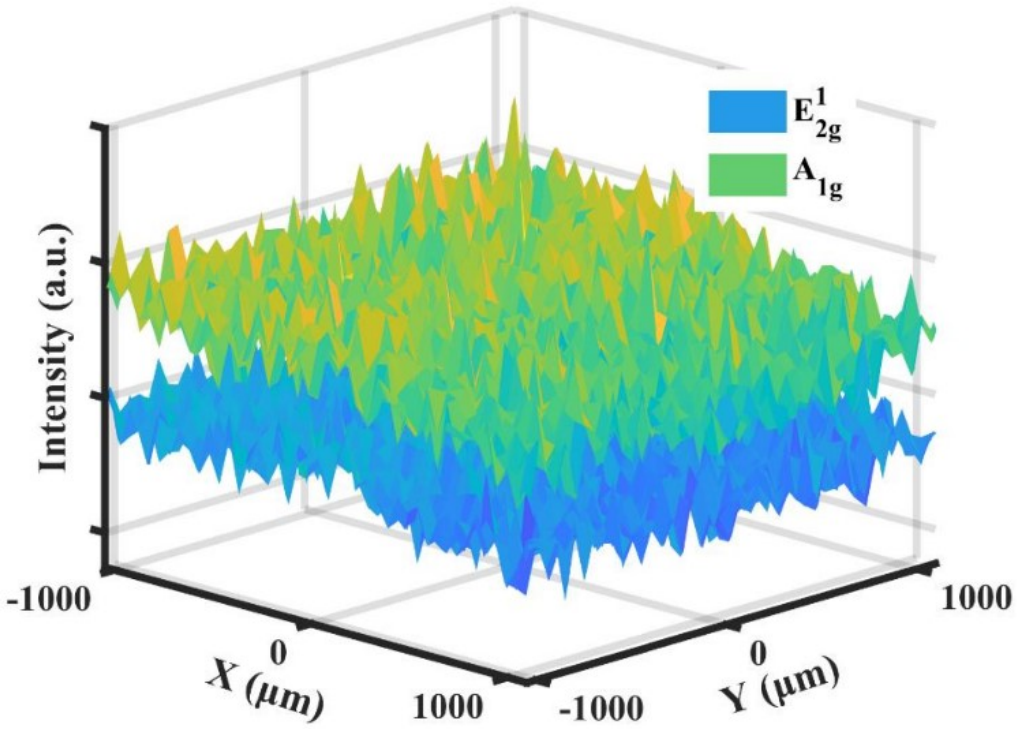

Figure.S1 Raman mapping of MoS_2 film. The mapping area is 2 mm × 2 mm, and each pixel is 50 μm × 50 μm in size. The standard deviations of the peak intensities of the mapping area are 9.8% (E^1_{2g} mode) and 8.5% (A^1_g mode), indicating the good uniformity of the device.

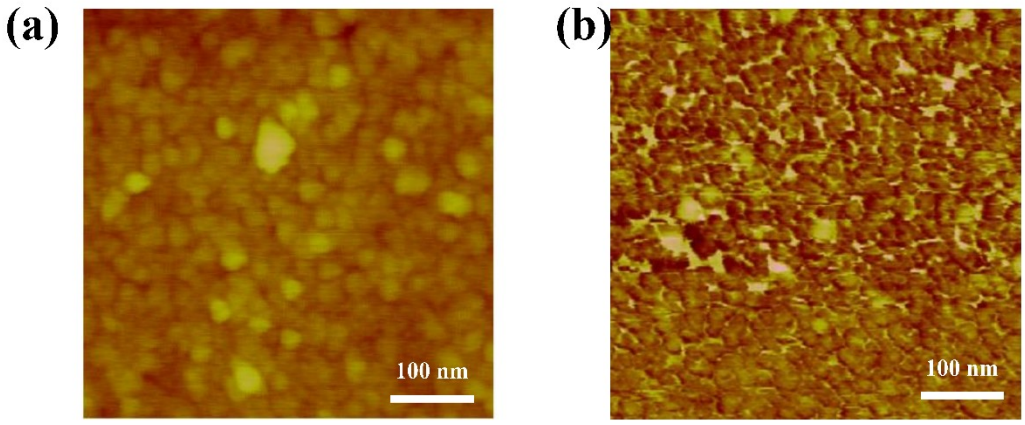

Figure.S2 AFM images of the MoS_2 film (a) before and (b) after annealing. The amorphous clusters were transformed into a flake-like polycrystalline state.

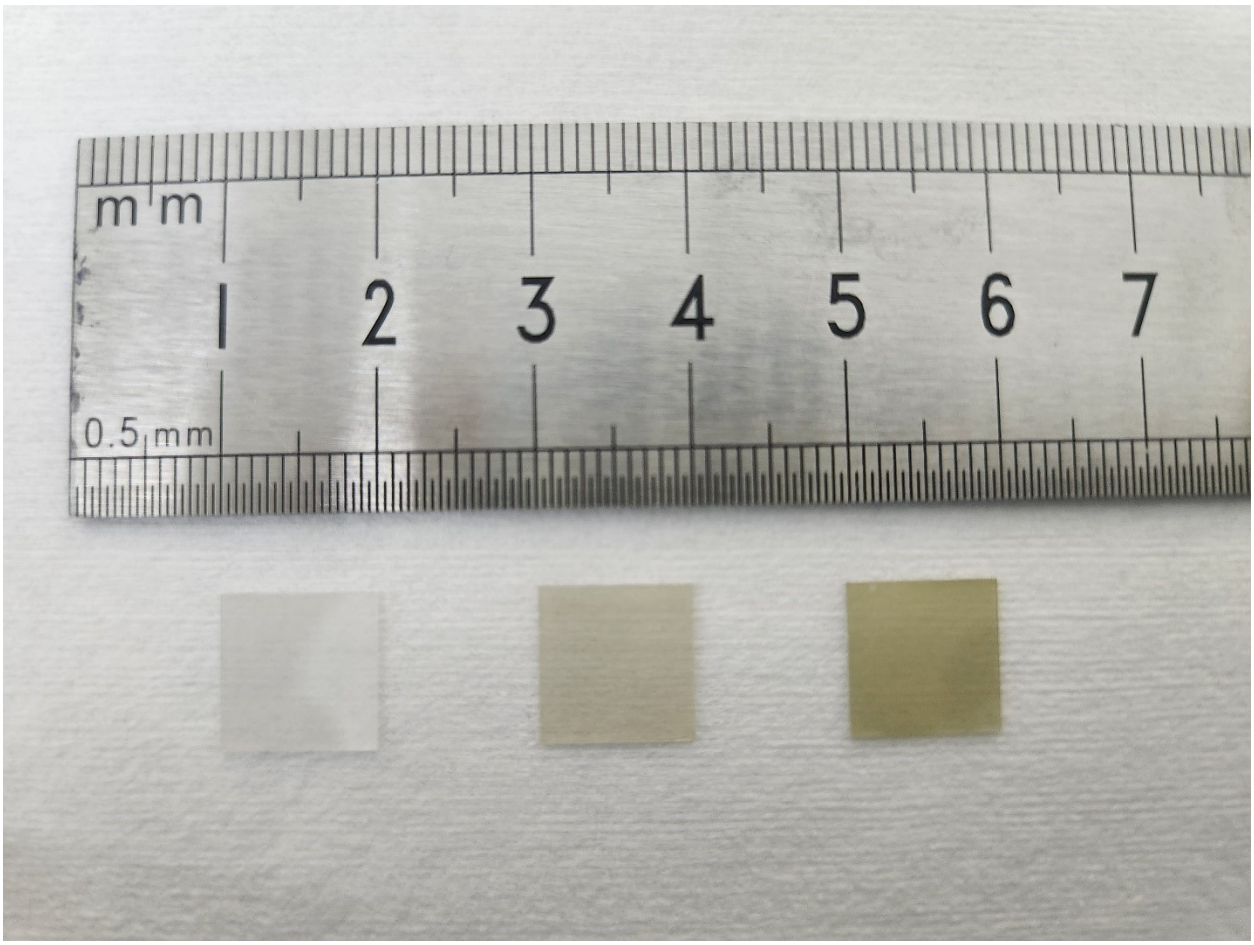

Figure.S3 Photo of sapphire substrate(left), MoS_2 film after 50 cycles growth(middle), MoS_2 film after 100 cycles growth(right), showing that the ALD process is highly uniform and controllable.

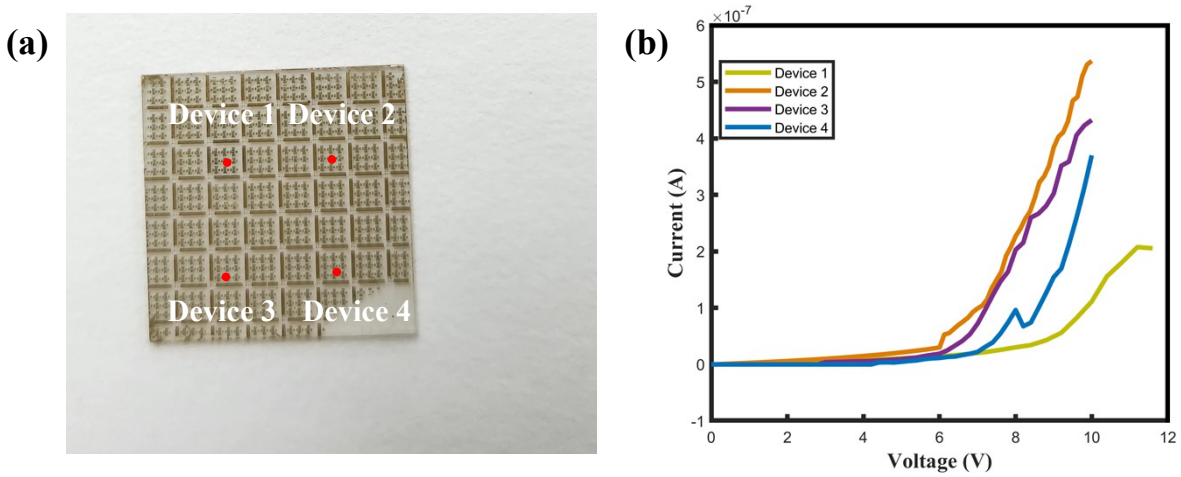

Figure.S4 Electroforming process characteristics of four independent devices.. (a) Photo of the devices (b) Electroforming process. The threshold voltage ranged from 6 V to 9 V, indicating that the electroforming process is commonly observed.

S2. Characterization of conductive filament.

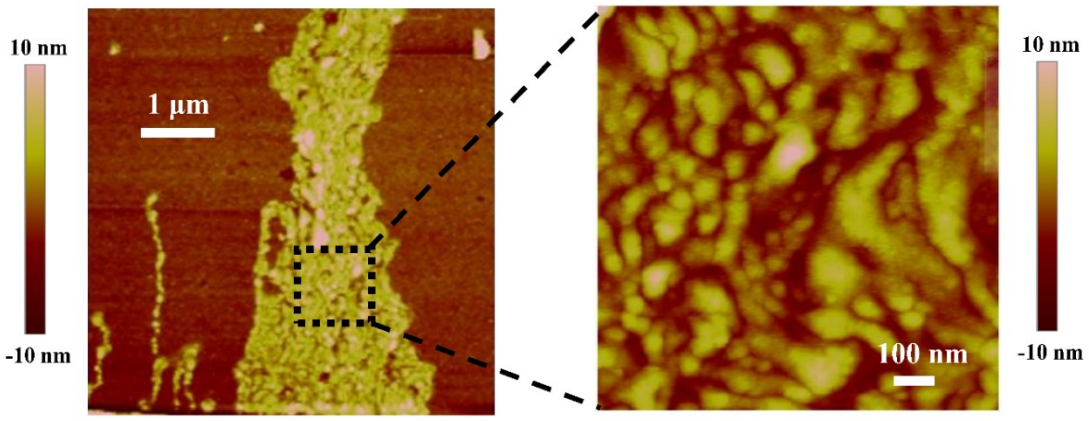

Figure.S5 AFM image of a conductive filament. The filament area bulges significantly and is much coarser than the outside area, which indicates that the electroforming of the conductive filaments disrupts the original lattice structure.

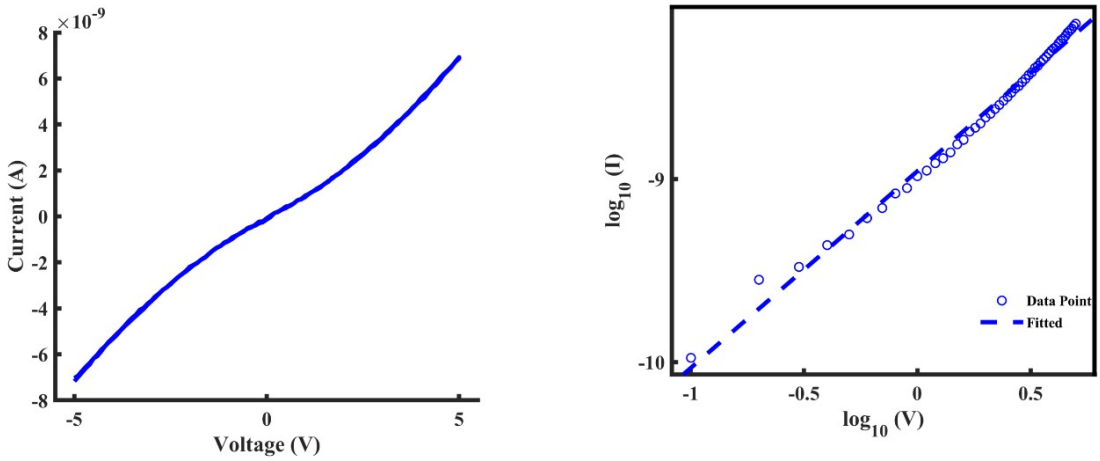

Figure.S6 (a) *I-V* curve of the device before electroforming and (b) log-log fitting of the curve. The slope of dotted line is 1.04, which indicates ohmic conduction in the pristine film.

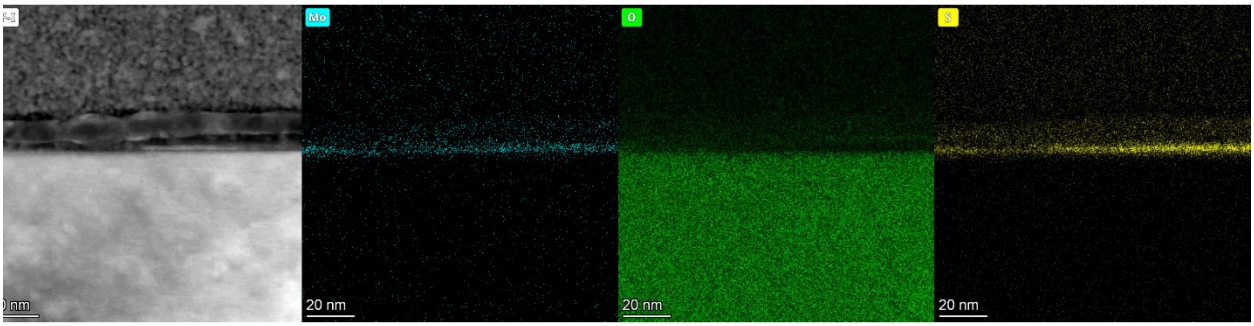

Figure.S7 HR-TEM image and EDS mapping of the edge of the filament area. The disappearance of the oxygen content gap and the reduction in the S content indicate the oxidation process (right side: pristine film; left side: filament area).

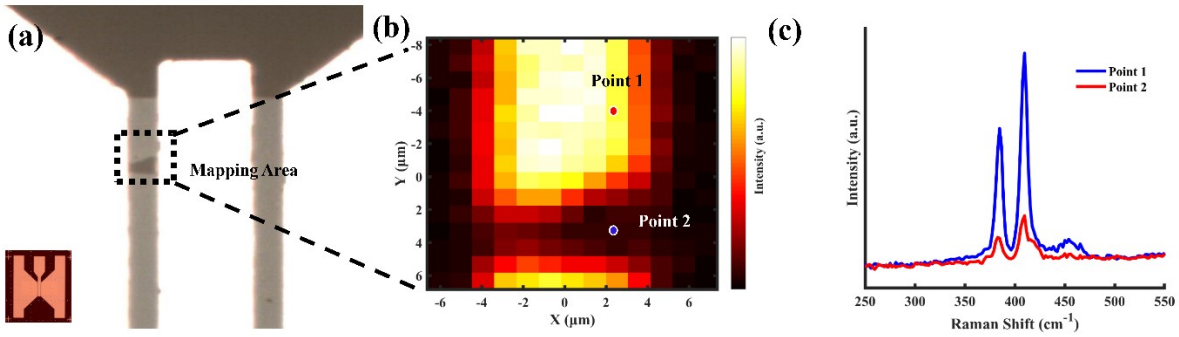

Figure.S8 (a) Optical image of the filament area. (b) Raman mapping of the filament area. (c) Raman spectra of the polycrystalline film and the filament area. The weakening of the peaks indicates the breaking of the Mo-S bonds.

S3. Synapse function of the device

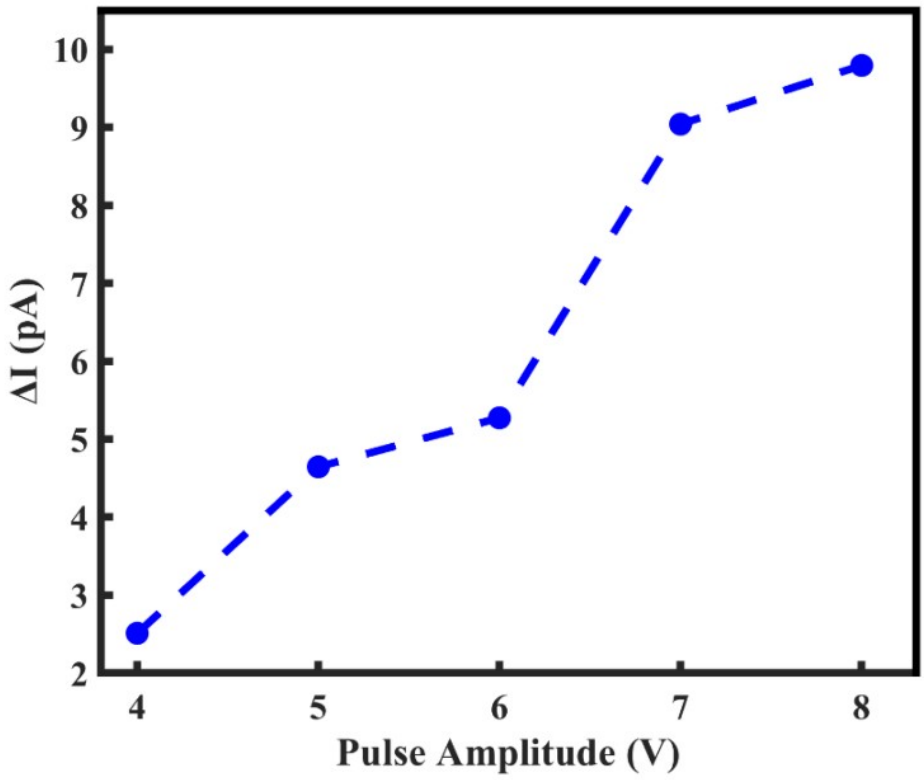

Figure.S9 Average conductance changes caused by single pulses with different amplitudes (4 V, 5 V, 6 V, 7 V, and 8 V).

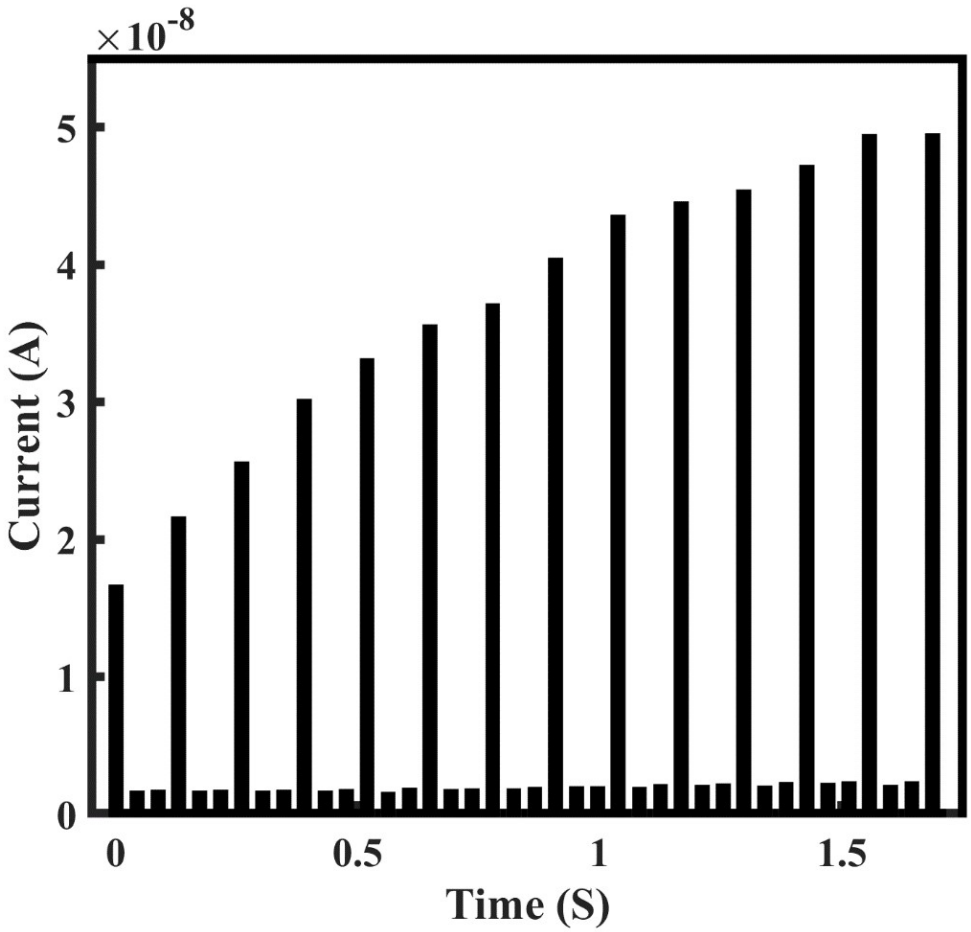

Figure.S10 Current changes during positive pulse potentiation. The magnitudes and widths of the stimulation pulses and the read pulses were set at 5 V/50 ms and 1 V/50 ms, respectively. The time interval between pulses was 50 ms. The power consumption of each set pulse/read pulse is lower than 0.25 μW/2 nW, respectively.

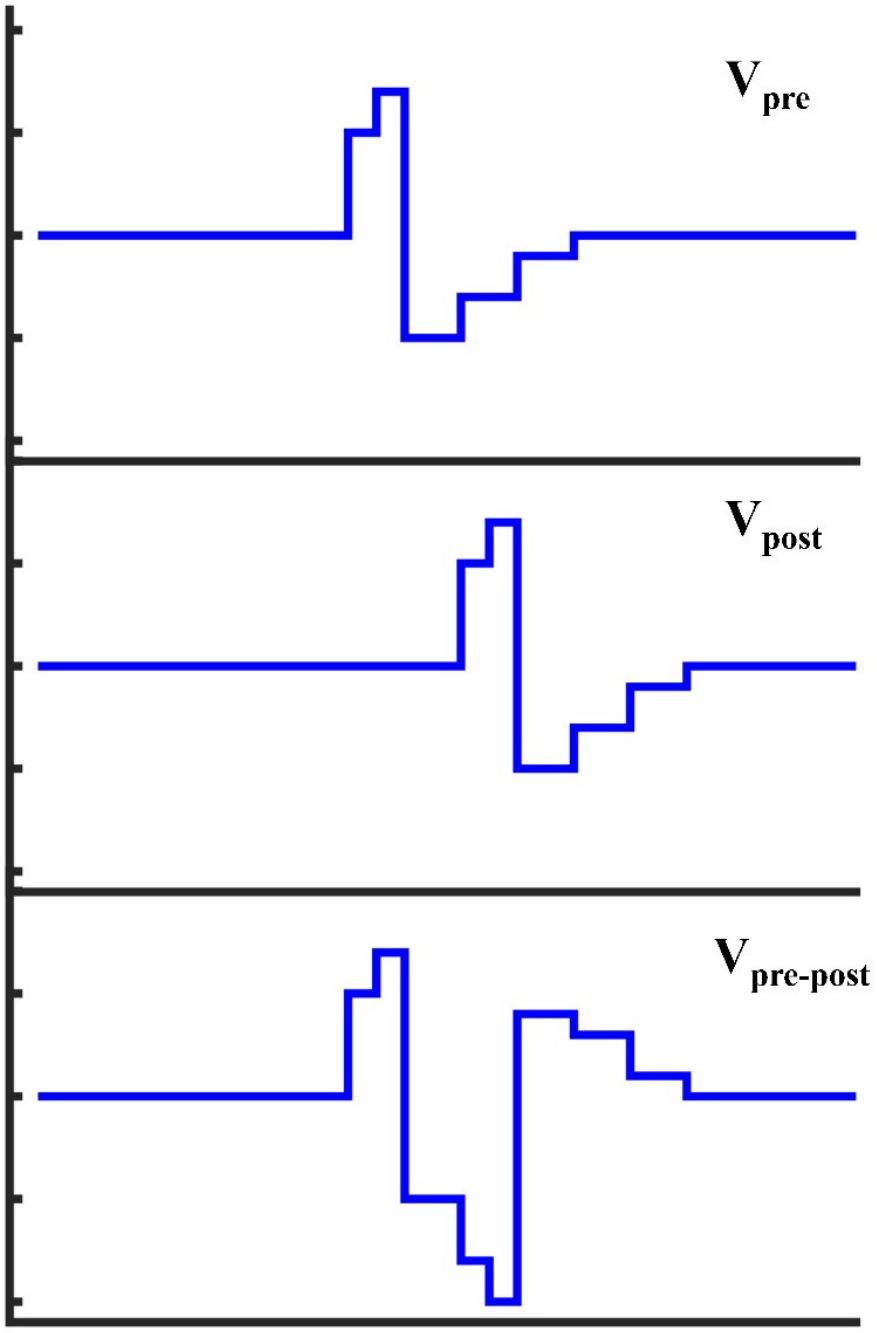

Figure.S11 Programmed pre- and postsynaptic pulses used to emulate STDP.

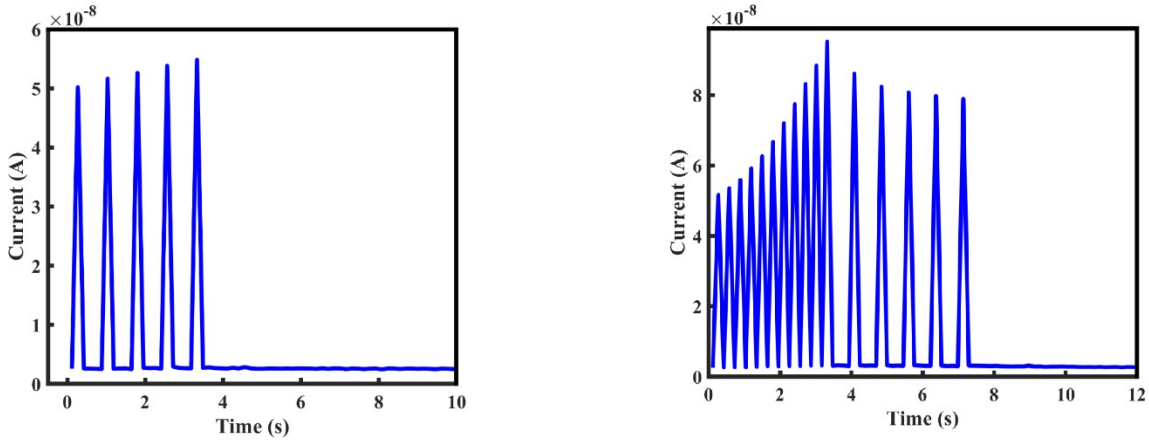

Figure.S12 Current responses to consecutive pulses after the device has been subjected to pulses at different frequencies. (a) Potentiation caused by five consecutive pulses (8 V, width of 0.2 s, interval of 0.6 s). (b) Depression caused by a second group of five consecutive pulses (8 V, width of 0.2 s, interval of 0.6 s) following the first five consecutive pulses (8 V, width of 0.2 s, interval of 0.1 s).